INSTITUTE OF PHYSICS PUBLISHING and INTERNATIONAL ATOMIC ENERGY AGENCY NUCLEAR FUSION

Nucl. Fusion **45** (2005) 1404–1410 doi:10.1088/0029-5515/45/11/022

Impurity-seeded ELMy H-modes in JET, with high density and reduced heat load

P. Monier-Garbet[1], Ph. Andrew[2], P. Belo[3], G. Bonheure[4], Y. Corre[5], K. Crombe[6], P. Dumortier[4], T. Eich[7], R. Felton[2], J. Harling[2], J. Hogan[8], A. Huber[9], S. Jachmich[4], E. Joffrin[1], H.R. Koslowski[9], A. Kreter[9], G. Maddison[2], G.F. Matthews[2], A. Messiaen[4], M.F. Nave[3], J. Ongena[4,10], V. Parail[2], M.E. Puiatti[11], J. Rapp[9,10], R. Sartori[12], J. Stober[7], M.Z. Tokar[9], B. Unterberg[9], M. Valisa[11], I. Voitsekhovitch[2], M. von Hellermann[13] and JET-EFDA contributors[a]

[1] Association EURATOM-CEA sur la Fusion Contrôlée, DSM/DRFC, Cadarache, St Paul-lez-Durance, France
[2] UKAEA/Fusion Association, Culham Science Center, Abingdon, OXON, UK
[3] Associaçao Euratom-IST, Centro de Fusao Nuclear, 1049-001 Lisbon, Portugal
[4] LPP-ERM/KMS, Euratom-Belgian State Association, TEC, Brussels, Belgium
[5] Association EURATOM-VR, Royal Institute of Technology, Physics Department, Stockholm, Sweden
[6] Department of Applied Physics, University of Gent, 9000 Gent, Belgium
[7] Max-Planck Institut für Plasmaphysik, Boltzmannstrasse, Garching, Germany
[8] Oak Ridge National Laboratory, USA
[9] Institut für Plasmaphysik, Forschungszentrum Jülich, EURATOM Association, TEC, Jülich, Germany
[10] EFDA, CSU Culham, Abingdon, OXON, UK
[11] Consorzio RFX—Associazione Euratom-Enea sulla Fusione, I-35127 Padova, Italy
[12] EFDA, CSU Garching, Garching, Germany
[13] FOM-Rijnhuizen, Ass. Euratom-FOM, PO Box 1207, 3430 BE Nieuwegein, The Netherlands[b]

E-mail: pascale.monier-garbet@cea.fr

Received 10 December 2004, accepted for publication 4 August 2005
Published 26 October 2005
Online at stacks.iop.org/NF/45/1404

Abstract

Experiments performed at JET during the past two years show that, in high triangularity H-mode plasmas with $I_p = 2.5$ MA, $n_e/n_{Gr} \approx 1.0$, it is possible to radiate separately up to ≈40% of the total injected power on closed flux surfaces in the pedestal region (argon seeding) and up to ≈50% of the injected power in the divertor region (nitrogen seeding), while maintaining the confinement improvement factor at the value required for ITER, $H98(y, 2) \approx 1.0$. The total radiated power fraction achieved in both cases (65–70%) is close to that required for ITER. However, Type I ELMs observed with impurity seeding have the same characteristics as that observed in reference pulses without seeding: decreasing plasma energy loss per ELM with increasing pedestal collisionality. One has to reach the Type III ELM regime to decrease the transient heat load to the divertor to acceptable values for ITER, although at the expense of confinement. The feasibility of an integrated scenario with Type-III ELMs, and $q_{95} = 2.6$ to compensate for the low H factor, has been demonstrated on JET. This scenario would meet ITER requirements at 17 MA provided that the IPB98 scaling for energy content is accurate enough, and provided that a lower dilution is obtained when operating at higher absolute electron density.

PACS numbers: 52.55.Rk, 52.25.Vy

1. Introduction

In ITER, both the steady-state and the transient heat flux to the divertor will have to be limited to values tolerable

[a] See appendix of Pamela J. *et al* 2003 Overview of JET results *Proc. 19th IAEA Fusion Energy Conf. (Lyon, 2002)* (Vienna: IAEA).
[b] Partner in the Trilateral Euregio Cluster (TEC).

for the wall materials ($<10\,\mathrm{MW\,m^{-2}}$ in steady-state, and $<50\,\mathrm{MJ\,m^{-2}\,s^{-1/2}}$ in transient conditions [1]). This paper reports on the experimental work performed at JET during the past two years to assess the feasibility of an integrated H-mode scenario using impurity seeding to reduce the heat flux to the divertor. A steady-state heat flux less than $10\,\mathrm{MW\,m^{-2}}$ in ITER is calculated to correspond to a total radiated power fraction $P_{\mathrm{rad,tot}}/P_{\mathrm{tot}} \approx 0.75$ (where $P_{\mathrm{rad,tot}}$ is the total radiated power, and P_{tot} the total input power), and in the present ITER scenario with C divertor and Be first wall, this is planned to be achieved using argon injection [2, 3], which for ITER pedestal parameters would correspond to high radiation in the divertor region, $P_{\mathrm{rad,div}}/P_{\mathrm{tot}} \approx 0.50$ ($P_{\mathrm{rad,div}}$ power radiated in the divertor region), and type I ELMs for good confinement. The 25% remaining radiation fraction is expected to come from bremsstrahlung losses in the bulk plasma with an effective charge $Z_{\mathrm{eff}} = 1.7$. The work reported here brings new insight into the following issues: (1) is it possible, in high triangularity, high density H-mode plasmas, to achieve $P_{\mathrm{rad,tot}}/P_{\mathrm{tot}} \approx 0.75$ together with good confinement? What are the respective contributions of bulk and divertor radiations in this case? What impurity species should be used to obtain this distribution? (2) What is the corresponding ELM regime? Can impurity be used to control/mitigate ELMs? A summary of the previous JET work on argon seeded H-modes is given in [4–6]. The experiments reported in these references were performed with the MkII-GB divertor configuration. High density ($n_{\mathrm{e}}/n_{\mathrm{Gr}} \geqslant 0.85$), confinement ($H98(y,2) \approx 1.0$) and β ($\beta_{\mathrm{N}} \geqslant 1.8$) were realized simultaneously together with a high radiation level. In low triangularity H-modes in the 'septum' configuration (x-point lying on the dome of the MkII-GB divertor), a peaking of the density profile was observed with argon injection, reminiscent of the observations made in the RI mode on TEXTOR [4]. The present work reports only on high triangularity ($\delta = 0.44$) plasmas with the MkII-SRP divertor configuration, without the septum. It advances the subject of heat load mitigation through two lines: first, it compares two radiating species, argon and nitrogen, both in terms of achieved radiated power and in terms of global confinement properties, with the aim of understanding from the experiment what are the characteristics of the impurity species that provide the best global plasma performances, in view of extrapolation to ITER. Second, the role of impurity seeding in the achieved performances is carefully assessed through a detailed comparison to a set of reference discharges without seeding. Previous JET work on nitrogen seeded H-modes is given in [7,8]. Similar studies performed on DIII-D are reported in [9], and on ASDEX-Upgrade in [10]. High performances with argon seeding and $n_{\mathrm{e}}/n_{\mathrm{Gr}} = 0.8$ are also obtained in JT60-U [11, 12], in a configuration close to the septum one on JET (the strike point on the dome top of the divertor).

2. Steady-state heat flux to the divertor and global confinement properties

2.1. Experimental conditions

Argon and nitrogen impurities have been injected in high density high triangularity H-mode plasmas in JET. In the argon seeding scenario, the radiated power and the confinement improvement factor are controlled simultaneously by the argon and deuterium injection rates through a feedback loop [13]. The plasma current and toroidal field are $I_{\mathrm{p}} = 2.5\,\mathrm{MA}$, $B_{\mathrm{t}} = 2.7\,\mathrm{T}$ corresponding to $q = 3.6$. The total injected power is $\approx$17 MW ($P_{\mathrm{NBI}} = 14\,\mathrm{MW} + P_{\mathrm{ICRH}} = 3\,\mathrm{MW}$). In the nitrogen seeding scenario, the nitrogen injection rate is either constant at a pre-set value, or is adjusted to control the radiated power through a feedback loop. A pre-set constant deuterium injection is used. The toroidal field is reduced to 2.0 T for $q = 2.6$ [7]. The total injected power is 13 MW. Figure 1 shows a few time traces for two typical pulses with argon seeding and nitrogen seeding. This paper compares the results of the argon and nitrogen experiments with the aim of determining the characteristics required for the seed impurity in ITER. Only high triangularity ($\delta = 0.44$) plasmas with the MkII-SRP divertor configuration, without the septum, are analysed. The best performance obtained so far with impurity seeding is compared with the corresponding JET 'reference' data base with no seeding [14].

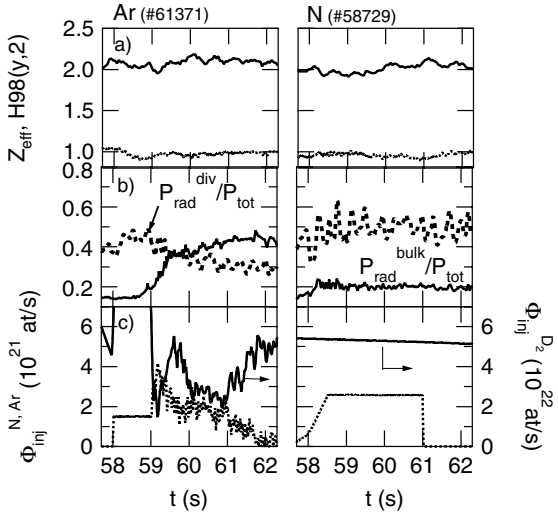

Figure 1. Comparison of a few time traces for two typical pulses with Ar seeding (left column) and N seeding (right column), in the same high triangularity configuration, the same fractions of Greenwald density ($n_{\mathrm{e}}/n_{\mathrm{Gr}} \sim 0.98$), and total radiated power fraction ($P_{\mathrm{rad}}^{\mathrm{tot}}/P_{\mathrm{tot}} \sim 0.70$). (*a*) Line averaged effective charge from visible bremsstrahlung measurements (——) and thermal confinement improvement factor calculated from the IPB98(y, 2) scaling law (· · · · · ·), (*b*) fraction of radiation in the divertor ($P_{\mathrm{rad}}^{\mathrm{div}}/P_{\mathrm{tot}}$, · · · · · ·) and inside the separatrix ($P_{\mathrm{rad}}^{\mathrm{bulk}}/P_{\mathrm{tot}}$, ——) and (*c*) argon, nitrogen and deuterium injection rates. The impurity injection rates (· · · · · ·) refer to the left axis. The deuterium injection rates (——) refer to the right axis.

2.2. Radiated power and thermal confinement

Figure 2 shows the thermal confinement improvement factor calculated from the IPB98(y,2) scaling law versus the electron density normalized to the Greenwald density (*a*), the total radiated power (*b*) and the power radiated in the divertor region (*c*) both normalized to the total injected power. The radiated power is measured by bolometry. The radiated power in the divertor region ($P_{\mathrm{rad,div}}$) shown in figure 2(*c*) corresponds to the poloidally asymmetric part of the radiation in the vicinity

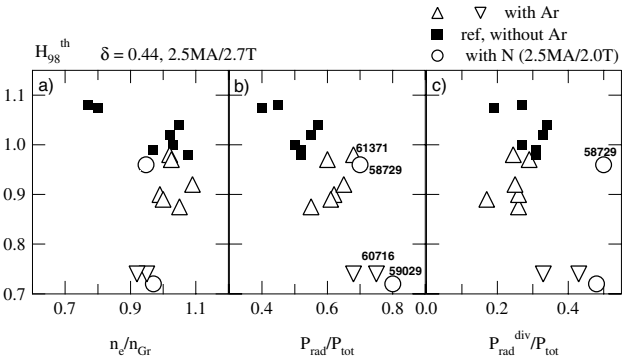

Figure 2. Thermal confinement factor versus (*a*) fraction of Greenwald density, (*b*) total radiated power fraction and (*c*) fraction of input power radiated in the divertor region. The upside down triangles correspond to pulses in which steady-state is not achieved. In a few cases, to refer easily to the text, the pulse numbers are written on the figure.

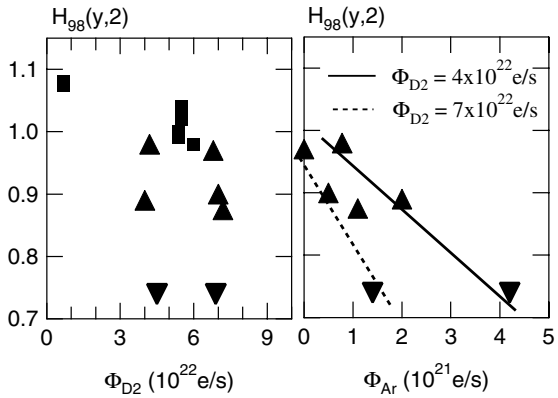

Figure 3. Left: Thermal confinement factor versus deuterium injection rate. ■: reference pulses with no impurity injection. ▲: pulses with a deuterium injection plus an argon injection (argon injection rate shown on the right figure). Right: thermal confinement factor versus argon injection rate for the same pulses as that shown on the left figure.

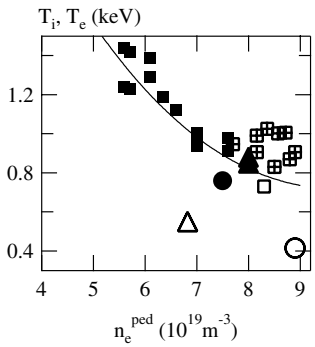

Figure 4. Pedestal (n_e, T_e) for high triangularity pulses at 2.5 MA/2.7 T. ■ = reference pulses (no impurity seeding), ▲ = Ar seeding, ● = *N* seeding. Full (○, △, □) symbols correspond to Type-I (Type-III) ELMs respectively. ⊞ refer to reference pulses with mixed TypeI/II ELMs.

of the X-point. It is the difference between the total radiated power ($P_{\mathrm{rad,tot}}$) and the contribution, which is poloidally symmetrical ($P_{\mathrm{rad,bulk}}/P_{\mathrm{tot}}$), and calculated from the bolometer lines of sight viewing the plasma upper half only. Analysis of the detailed tomographic reconstruction of bolometry data indicates that the determination of $P_{\mathrm{rad,div}}$ and $P_{\mathrm{rad,bulk}}$ as reported above is accurate within ±10%. Further analysis of the radiation patterns observed with argon or nitrogen seeding is reported in section 2.3 below. The reference data base obtained in high density high triangularity H-modes with no seeding shows that in JET, with carbon divertor and first walls, $P_{\mathrm{rad,div}}/P_{\mathrm{tot}} \approx 0.30$ and $P_{\mathrm{rad,bulk}}/P_{\mathrm{tot}} \approx 0.25$ (total radiated power fraction $P_{\mathrm{rad,tot}}/P_{\mathrm{tot}} \approx 0.55$) are currently achieved with $H98(y,2) = 1.0$–1.05. With either argon or nitrogen seeding, a total radiated power fraction $P_{\mathrm{rad,tot}}/P_{\mathrm{tot}}$ up to 0.65–0.70 (#61371 and #58729) is achieved with a confinement loss limited to ≈5% ($H98(y,2) \sim 1.0$) compared to the best reference H-modes. Consistent with bolometry data, infrared measurements of the inner target plate surface temperature also indicate a lower heat flux to the inner plate in the impurity seeded scenario, compared with the non-seeded case. Increasing the radiated power fraction beyond 0.65–0.70 leads to further degradation of the confinement (#60716 and #59029 for argon and nitrogen, respectively). Figure 3 analyses the separate effects of deuterium and impurity injection rates on confinement, in argon seeded plasmas. It shows that (i) the global confinement decreases with increasing argon injection rate; (ii) it decreases more rapidly in the case of a high deuterium injection ($\Phi_{D_2} = 7 \times 10^{22}\,\mathrm{e\,s^{-1}}$ compared with $\Phi_{D_2} = 4 \times 10^{22}\,\mathrm{e\,s^{-1}}$), which is consistent with these different rates producing very similar electron densities in the plasma; (iii) even in the case of a low argon injection, corresponding to discharges in which $H98(y,2)$ is still close to 1.0, the 5% confinement loss in these pulses is correlated to the impurity injection and may not be attributed to a strong deuterium injection.

The degradation of the global confinement observed at high radiated power fractions is correlated with a decrease of the pedestal electron temperature, as illustrated by the pedestal (T_e, n_e) diagram (figure 4). A total radiated power fraction ⩾0.75–0.80, either with argon or nitrogen radiation brings the pedestal temperature well below the level usually observed in good H-mode confinement pulses. The transition towards lower confinement occurs at a higher value of $P_{\mathrm{rad,bulk}}/P_{\mathrm{tot}}$ (≈40%) with argon than with nitrogen (≈20%) since, due to its atomic physics characteristics, argon radiates mainly in the region where $T_e \geqslant 900\,\mathrm{eV}$, which corresponds to the pedestal temperature for Type I ELMs and good confinement. On the other hand, nitrogen radiates at a lower electron temperature, well within the domain for Type III ELMs. In the high confinement regime with Type I ELMs, the electron temperature profiles, inside the pedestal region, are very similar in cases without and with impurity seeding (figure 5). This is consistent with the observation shown on figure 6, that at a given value of the total stored plasma energy (W), the ratio of the pedestal energy (W_{ped}) to the total stored energy (W) is the same in seeded and non-seeded discharges (W_{ped}/W changes linearly with W, and the data for impurity injection follow the same trend as the reference data with no injection). This indicates that these impurity seeded pulses do not break the link between the global confinement and the pedestal properties, which is usually observed in JET H-modes. This result is different from that reported from JT60-U [11, 12], at

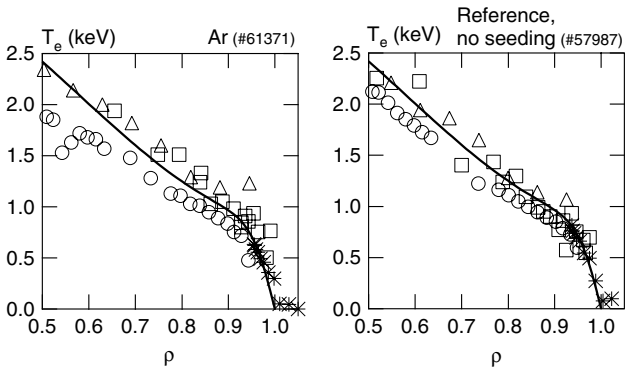

Figure 5. Electron temperature profiles of two pulses shown in figure 2, with $H98(y,2) = 1.0$ and Type I ELMs, with argon seeding (left), and without impurity seeding (reference pulse, right). ○: electron temperature from ECE data; △: LIDAR Thomson scattering data; ⚹: edge LIDAR Thomson scattering; □: charge exchange recombination spectroscopy. The solid line is a fit through the data.

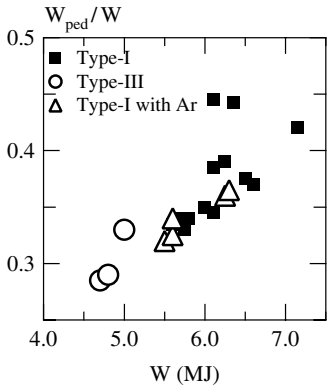

Figure 6. Fraction of pedestal energy for reference pulses without seeding, and for argon seeded pulses. High triangularity configuration ($\delta \geqslant 0.4$). At a given value of the total stored plasma energy (W), the fraction of energy in the pedestal is the same for seeded and non-seeded discharges.

lower values of n_e/n_{Gr}, and with a different divertor geometry, where higher electron and ion temperatures were found in the pedestal region and higher gradients of the temperature were found in the core. The ELM regimes observed in our series of experiments on JET, for $P_{rad,tot}/P_{tot} \leqslant 0.70$ ($H98(y,2) \approx 1.0$) and $P_{rad,tot}/P_{tot} \geqslant 0.75$ (low confinement) will be discussed in section 3. With nitrogen seeding, at the highest achieved radiated power fractions, partially detached divertor conditions are observed. The heat flux density is reduced to about 2–5 MW m^{-2} and electron temperatures in the divertor of less than 10 eV are achieved [8]. The reduced normalized confinement observed in these conditions is proposed to be compensated in ITER by operating at high plasma current, $I_p = 17$ MA. Indeed, the ITER operational domain for $Q = 10$ does allow operation at confinement enhancement factors of $H98(y,2) \approx 0.78$ provided the plasma current is increased accordingly. Pulse 59029 shown in figure 2 demonstrates on JET the feasibility of such an integrated scenario: 2.5 MA/2.0 T, $q_{95} = 2.6$, $H98(y,2) = 0.73$, $P_{rad,tot}/P_{tot} = 0.80$, $n_e/n_{Gr} = 1.0$, $Z_{eff} = 2.1$, $\beta_N = 1.7$, $\delta = 0.44$) [7, 8].

2.3. Comparison of argon and nitrogen radiation patterns

Figure 7 shows the radiation patterns, obtained from tomographic reconstruction of bolometry data, of two H-mode pulses with very similar global characteristics, in particular $H98(y,2) \approx 1.0$, Type I ELMs, $P_{rad,tot}/P_{tot} = 0.65$–$0.70$, except that the seed impurity is different in the two pulses (time traces shown in figure 1). In the case of argon seeding, most of the radiation is emitted on closed flux surfaces inside the separatrix ($P_{rad,bulk}/P_{tot} \approx 0.40$) and ≈25% of the total power is radiated in the divertor region. In contrast, with nitrogen seeding, most of the radiation is located in the divertor region, $P_{rad,div}/P_{tot} \approx 0.50$. The radial profiles of the radiated power density from tomographic reconstruction of the bolometry data are shown in figure 8, together with the corresponding electron temperature profiles. In the case of argon seeding, the radiative shell extends in the edge region for $\rho > 0.5$ and $T_e < 2.0$ keV, in good qualitative agreement with the radiation of Ar XVI ions at coronal equilibrium. The average effective charge measured by visible bremsstrahlung is very similar in the two discharges, $Z_{eff} \approx 2.1$ either with argon or nitrogen seeding. Spectroscopic measurements show that, at these high radiative power fractions, the carbon influx from the divertor is reduced significantly with nitrogen seeding [8]. The intrinsic impurities, mainly C and Be, are replaced by the seed impurity. The resulting core nitrogen concentration measured by charge exchange recombination spectroscopy reaches ∼1.5%. The argon concentration (roughly estimated from Z_{eff}) is in the range 0.3–0.4%. A detailed modelling of the plasma impurity content and of the power radiated by each impurity species is in progress.

3. Transient heat flux to the divertor during ELMs

3.1. Scaling of Type I ELMs plasma energy loss in impurity seeded plasmas

Type I and Type III ELM regimes are observed for $P_{rad,tot}/P_{tot} \leqslant 0.70$ ($H98(y,2) \approx 1.0$) and $P_{rad,tot}/P_{tot} \geqslant 0.75$ (low confinement), respectively. This is true for argon and for nitrogen impurities. The precise value of $P_{rad,tot}/P_{tot}$ at the Type I/III transition is difficult to determine from the available experimental data. In particular, it is not possible to determine from the limited data base analysed here, whether there is a difference between argon and nitrogen, although a higher value of $P_{rad,tot}/P_{tot}$ at the Type I/III transition would be expected with nitrogen since it corresponds to a lower power loss channel in the pedestal region. Analysis made so far shows that the Type I ELMs observed with impurity seeding have the same characteristics as that observed in the reference high triangularity pulses without seeding (figure 9). In particular, the plasma energy loss per ELM, $\Delta W_{ped}/W_{dia}$, decreases with increasing pedestal collisionality [6, 7], following the empirical scaling found in [3]. These results show that impurity seeding may be used as an additional tool to control the pedestal collisionality, at the expense of a reduced pedestal temperature. The frequency of the Type I ELMs observed with argon seeding decreases with increasing $P_{rad,bulk}$, i.e. decreasing conductive power across the separatrix. Predictive modelling with the JETTO code shows that the decreased frequency is due to a decreased power across

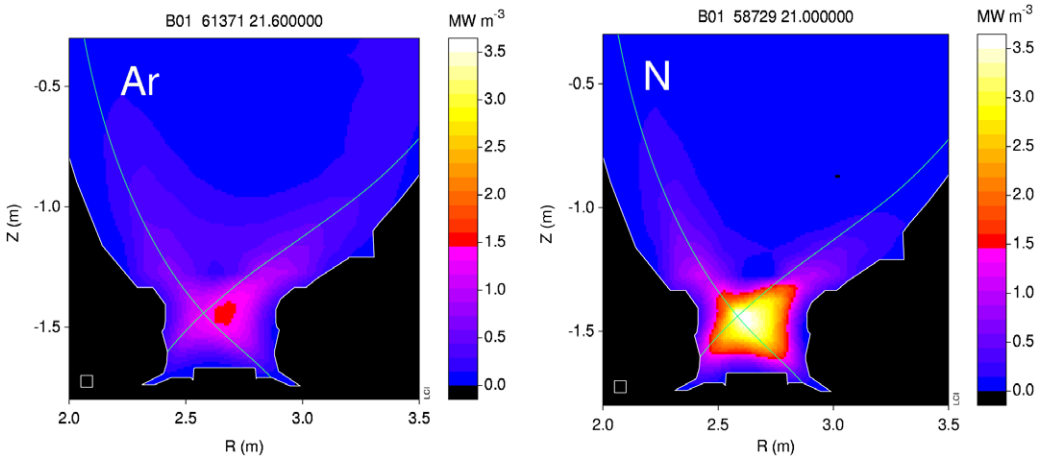

Figure 7. Bolometric reconstruction of the radiated power density in the X-point region for the two pulses shown in figure 1(*a*) with argon seeding, and (*b*) with nitrogen seeding.

(This figure is in colour only in the electronic version)

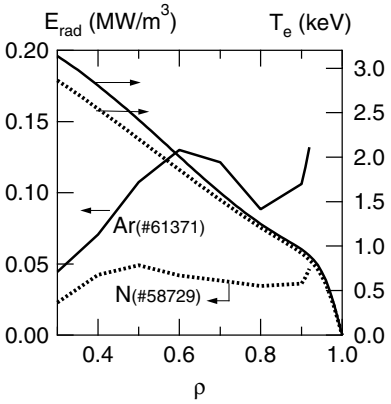

Figure 8. Radial profiles of the radiated power density for the two pulses shown in figure 7. These profiles are obtained from tomographic reconstruction of bolometer data. The electron temperature profiles are shown on the right axis. Argon seeded pulse: ——. Nitrogen seeded pulse: · · · · · ·.

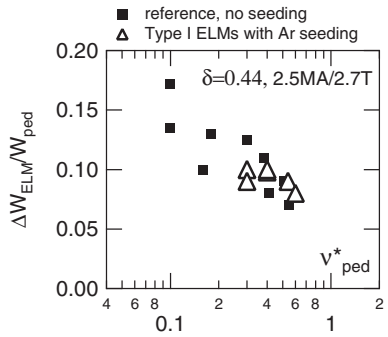

Figure 9. Normalized plasma energy loss per ELM versus pedestal collisionality for high triangularity H-mode pulses with Type I ELMs. ■: reference pulses without seeding. △: Ar seeded H-modes.

the separatrix rather than a higher threshold for ballooning instability which might have been associated to increased $Z_{\rm eff}$. Similar results on the influence of impurity seeding on ELM activity are reported from ASDEX-Upgrade [15], or from JT-60U [12].

3.2. Radiation buffering of Type I ELMs

Experimental work has also been done on JET [16] to determine whether the fraction of the released ELM energy that reaches the target plates could be reduced through enhanced radiation in the Scrape Off Layer (SOL) and divertor regions in conditions where an additional impurity is injected into the plasma edge. ('buffering' effect). For diagnostic purposes, these experiments have been done in a low triangularity shape plasma ($\delta\sim$ 0.26). N or Ar impurities are injected in Type-I ELMy H-modes up to a radiative power fraction of ∼55%. The heat load to the target plates, during and in between ELMs, is measured using a fast infra-red camera [17]. The presence of a co-deposited layer on the inner target is taken into account to calculate the deposited energy and heat fluxes from the surface temperature measurement [18]. The Type I ELMs analysed here correspond to $\Delta W_{\rm dia}$ up to 500 kJ. Figure 10 shows the energy increase on the target plate during an ELM, versus the corresponding plasma energy loss in two cases: a reference case without impurity seeding (solid squares, and linear fit shown by the solid line), and in cases where the radiation in the SOL has been increased through N or Ar seeding (open symbols, dashed line). It indicates that: (1) even in the reference case, less than ∼70% $((\Delta W_{\rm outer\ target} + \Delta W_{\rm inner\ target})/\Delta W_{\rm dia})$ of the released ELM energy reaches the target plates. The 'missing' energy might either be radiated in the SOL or deposited on the vessel walls by perpendicular transport. (2) this fraction is only marginally reduced (by 18–24% on the outer and inner targets, respectively) when an additional impurity is puffed into the plasma edge, indicating that there is no additional dissipation of the released ELM energy in that case. Only at very high radiative power fractions (>80%) obtained with N seeding, experimental evidence of buffering of small type III ELMs is found when complete detachment in between ELMs is achieved [8], and both the transient power load to the divertor and the plasma energy loss due to ELMs are decreased (Type III ELM regime, $\Delta W_{\rm dia} \sim 25$ kJ, $\Delta W/W \sim 0.7\%$).

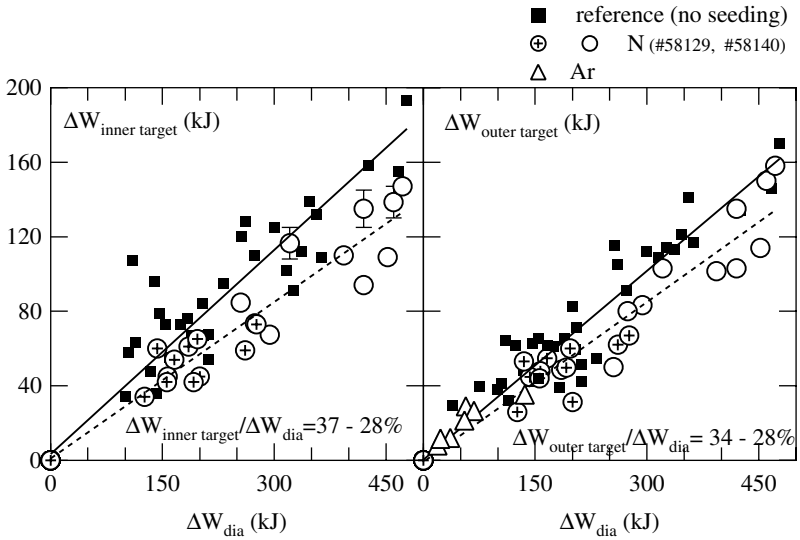

Figure 10. Energy increase on the inner (left) and outer (right) divertor targets versus plasma energy loss during a Type I ELM. ■: reference case without seeding. The solid line is a linear fit through these reference data. △, ○, ⊕: corresponding data when edge radiation is increased (up to ∼55% radiated power fraction) through N or Ar seeding. The dashed line is a linear fit through the data with impurity seeding. ○: pedestal density, $n_e^{ped} = 3.7 \times 10^{19}\,m^{-3}$; ⊕: $n_e^{ped} = 5.0 \times 10^{19}\,m^{-3}$, △: $n_e^{ped} = 7.0 \times 10^{19}\,m^{-3}$.

3.3. Modelling

The above experimental results are supported by time-dependent SOLPS5.0/B2-EIRENE modelling [19]. The core plasma is described using the MIST and SANCO impurity transport codes. These include an ELM model in which impurities are assumed to be instantaneously expelled into the SOL from the ELM-affected region and then recycled. The edge region (both the SOL and pedestal) is modelled using the time-dependent SOLPS5.0/B2-EIRENE code. SOLPS5.0/B2-EIRENE is a coupled 2D fluid plasma Monte-Carlo neutrals code, similar to EDGE2D-NIMBUS or UEDGE, the two other self-consistent 2D edge codes that are used to simulate JET shots. A comparison of these three codes is given in [19]. Deuterium plus two impurity species, C and N, are included. The ELMs are described by increased heat and particle perpendicular diffusivities compared with steady-state values. Enhancement factors of 50 and 100 have been used: these values correspond to the same ELM energy loss in the experiment (there is a fixed amount of ΔW_{dia} which can be removed, 350–400 kJ in the case considered), but the higher enhancement case removes the energy faster, and the time to remove it is smaller. Figure 11 shows the calculated electron energy hitting the divertor target normalized to that crossing the separatrix, versus the time needed to remove the energy from the pedestal (τ_{ELM}, determined by the enhancement factor). The calculation is shown for a reference plasma with no seeding (open triangles, #58135 reference case without impurity seeding), and for a case with N seeding (solid triangles, #58139). Although the calculated fraction of the ELM energy reaching the target is smaller than that actually observed, the reduction of ≈15% of $\Delta W_{target}/\Delta W_{SOL}$ with N seeding which is calculated for $\tau_{ELM} \approx 150\,\mu s$ is consistent with the experimental findings, and with previous code results [3, 7], predicting that a significant effect could only be obtained for very small ELMs ($\Delta W_{dia} < 0.6$ MJ in ITER). Note that a stronger reduction is predicted for a longer ELM.

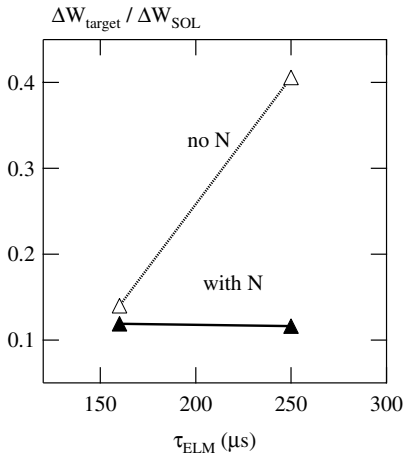

Figure 11. Integrated electron energy on the target plate normalized to that in the SOL versus time needed to remove a given energy from the pedestal. Solps 5.0 calculation for #58135 (without N) and #58139 (with N).

4. Conclusion

4.1. Steady-state heat flux to the divertor

Analysis of JET high triangularity H-mode experiments with $I_p = 2.5$ MA, $n_e/n_{Gr} \approx 1.0$ shows that, provided the appropriate impurity species is chosen, Ar and N, respectively, for JET plasma conditions, it is possible to radiate separately up to ≈40% of the total injected power on closed flux surfaces in the pedestal region and up to 50% of the injected power in the divertor region, while maintaining the confinement factor close to that required for ITER. In both cases, $P_{rad,tot}/P_{tot} \approx$ 0.65–0.70. Increasing the radiation level above this value leads to a degradation of the pedestal parameters, Type III ELM regime, and reduced confinement. Indeed, the increase

in radiation is associated with a reduced pedestal energy, and the fraction of energy in the pedestal (W_{ped}/W_{tot}) is the same, for a given confinement level, with and without impurity seeding. Predicting the corresponding maximum values of $P_{rad,bulk}/P_{tot}$ and $P_{rad,div}/P_{tot}$ achievable in ITER together with good confinement remains however uncertain, as the relation between divertor and pedestal electron density and temperature is different in JET and ITER, and the non-dimensional parameters of the experiments analysed here are not that of ITER plasmas. In this respect, experiments in JET at higher plasma current ($\geqslant$3.0 MA), and consequently higher absolute density, would bring valuable additional information on the scaling with current and input power of the limits in $P_{rad,bulk}/P_{tot}$ and $P_{rad,div}/P_{tot}$, which are achievable with good confinement. Another option to be explored in order to increase further the radiated power and maintain the confinement could be to increase the actual volume used for radiation by combining two impurity species, one radiating at the temperature of the top of the pedestal to produce $P_{rad,bulk}/P_{tot} \leqslant 0.40$, and the other one radiating at lower temperature, in the divertor region to produce $P_{rad,div}/P_{tot} \leqslant 0.50$. However, for the scenario involving high radiation on closed flux surfaces inside the separatrix, two further issues have still to be assessed carefully: the proximity of the H to L power threshold ($P_{L-H} \propto n_e$), and the net decrease of heat flux to the divertor that the scenario would bring (higher injected power, to compensate for the power radiated inside the separatrix).

4.2. Transient heat flux to the divertor during Type I ELMs

As shown in figure 4, the operational domain with impurity seeding and good confinement corresponds to the Type I ELM domain. The normalized plasma energy loss ($\Delta W_{dia}/W_{ped}$) during Type I ELMs follows the same scaling with the pedestal collisionality, without and with impurity seeding. Infrared thermography measurements show that, in the reference H-modes without impurity seeding, less than 70% of the released Type I ELM energy reaches the target plate, and this fraction is only marginally reduced when an additional impurity is injected into the plasma edge (no additional radiation 'buffering' of Type I ELMs is observed). In conclusion, there is no experimental evidence so far of any strong reduction of the transient heat flux to the divertor during Type I ELMs with impurity seeding. One has to reach the Type III ELM regime to decrease the transient heat load to the divertor to acceptable values for ITER.

Finally, on the basis of the experimental results discussed above, two options using impurity seeding may be further considered for an integrated scenario for ITER: (1) use impurity injection to obtain $P_{rad,tot}/P_{tot} \approx 0.75$ with $H98(y,2) \approx 1.0$, but one needs a separate technique to mitigate the Type I ELMs, (2) use a Type III ELM regime with impurity seeding, to obtain sustainable steady-state and transient heat loads to the divertor, although at the expense of confinement. The feasibility of such an integrated scenario has been demonstrated on JET: 2.5 MA/2.0 T, $q_{95} = 2.6$, $H98(y,2) = 0.73$, $P_{rad,tot}/P_{tot} = 0.80$, $n_e/n_{Gr} = 1.0$, $Z_{eff} = 2.1$, $\beta_N = 1.7$, $\delta = 0.44$) [7]. It would meet ITER requirements at 17 MA provided that the ITER98 scaling for energy content is accurate enough, and provided that a lower dilution is obtained when operating at higher absolute electron density.

References

[1] Federici G. *et al* 2003 *J. Nucl. Mater.* **313–316** 11–22
[2] Kukushkin A.S. and Pacher H.D. 2002 *Plasma Phys. Control. Fusion* **44** 931–43
[3] Loarte A. *et al* 2000 *Proc. 18th Int. Conf. on Fusion Energy 2000 (Sorrento, 2000)* (Vienna: IAEA) CD-ROM file ITERP/11(R) and http://www.iaea.org/programmes/ripc/physics/fec2000/html/node1.htm
[4] Ongena J. *et al* 2001 *Phys. Plasmas* **8** 2188
[5] Dumortier P. *et al* 2002 *Plasma Phys. Control. Fusion* **44** 1845–61
[6] Maddison G. *et al* 2003 *Plasma Phys. Control. Fusion* **45** 1657
[7] Rapp J. *et al* 2004 *Nucl. Fusion* **44** 312–19
[8] Rapp J. *et al* 2005 *J. Nucl. Mater.* **337–339** 826–30
[9] Wade M.R. *et al* 1999 *J. Nucl. Mater.* **266–269** 44
[10] Gruber O. *et al* 1995 *Phys. Rev. Lett.* **74** 4217
[11] Kubo H. *et al* 2001 *Nucl. Fusion* **41** 227
[12] Kubo H. *et al* 2002 *Phys. Plasmas* **9** 2133
[13] Dumortier P. *et al* 2004 Trace tritium experiments in high performance feedback controlled Ar seeded high triangularity ELMy H-mode discharges in JET *Proc. 31st EPS Conf. (28 June–2 July 2004, London)* P5.170
[14] Sartori R. *et al* 2002 *Plasma Phys. Control. Fusion* **44** 1801–13
[15] Suttrop H. 1998 *Plasma Phys. Control. Fusion* **40** 771
[16] Monier-Garbet P. *et al* 2003 Assessment of the use of injected impurities for heat flux mitigation in JET ELMy H-modes *30th EPS Conf. on Controlled Fusion and Plasma Physics (St Petersburg, Russia, 7–11 July 2003)*
[17] Eich Th. *et al* 2003 *J. Nucl. Mater* **313–316** 919–24
[18] Corre Y. *et al* 2003 Assessment of heat flux deposition and surface layer properties based on infrared measurements in JET experiments *30th EPS Conf. on Controlled Fusion and Plasma Physics (St Petersburg, Russia, 7–11 July 2003)*
[19] Coster D. *et al* 2003 *J. Nucl. Mater.* **313–316** 868